



Contents lists available at ScienceDirect

## Bioorganic &amp; Medicinal Chemistry Letters

journal homepage: [www.elsevier.com/locate/bmcl](http://www.elsevier.com/locate/bmcl)

## 7-Azaindole-3-acetic acid derivatives: Potent and selective CRTh2 receptor antagonists

David A. Sandham<sup>a,\*</sup>, Claire Adcock<sup>a</sup>, Kamlesh Bala<sup>a</sup>, Lucy Barker<sup>b</sup>, Zarin Brown<sup>b</sup>, Gerald Dubois<sup>b</sup>, David Budd<sup>b</sup>, Brian Cox<sup>a</sup>, Robin A. Fairhurst<sup>a</sup>, Markus Furegati<sup>c</sup>, Catherine Leblanc<sup>a</sup>, Jodie Manini<sup>b</sup>, Rachael Profit<sup>b</sup>, John Reilly<sup>a</sup>, Rowan Stringer<sup>b</sup>, Alfred Schmidt<sup>c</sup>, Katharine L. Turner<sup>a</sup>, Simon J. Watson<sup>a</sup>, Jennifer Willis<sup>b</sup>, Gareth Williams<sup>b</sup>, Caroline Wilson<sup>b</sup>

<sup>a</sup> Global Discovery Chemistry, Novartis Institutes of Biomedical Research, Horsham Research Centre, Wimblehurst Road, Horsham, West Sussex RH12 5AB, United Kingdom

<sup>b</sup> Respiratory Diseases Area, Novartis Institutes of Biomedical Research, Horsham Research Centre, Wimblehurst Road, Horsham, West Sussex RH12 5AB, United Kingdom

<sup>c</sup> Global Discovery Chemistry, Novartis Institutes of Biomedical Research, Postfach CH-4002, Basel, Switzerland

### ARTICLE INFO

#### Article history:

Received 29 May 2009

Revised 10 June 2009

Accepted 11 June 2009

Available online 14 June 2009

#### Keywords:

CRTh2

Prostaglandin D<sub>2</sub>

Azaindole

Eosinophils

Allergic diseases

### ABSTRACT

High throughput screening identified a 7-azaindole-3-acetic acid scaffold as a novel CRTh2 receptor antagonist chemotype, which could be optimised to furnish a highly selective compound with good functional potency for inhibition of human eosinophil shape change in whole blood and oral bioavailability in the rat.

© 2009 Elsevier Ltd. All rights reserved.

Prostaglandin D<sub>2</sub> (PGD<sub>2</sub>), a product of the arachidonic acid cascade, is synthesized primarily by mast cells, as well as by macrophages and Th2 lymphocytes. PGD<sub>2</sub> has long been associated with the allergic inflammatory response, being found at high concentrations in the lungs of asthmatic patients.<sup>1</sup> PGD<sub>2</sub> was initially believed to act solely through the DP receptor, although more recently a second receptor for PGD<sub>2</sub>, known as CRTh2 or DP<sub>2</sub> has been identified.<sup>2</sup> CRTh2 shows minimal homology with DP and is expressed on inflammatory cells, in particular showing selective expression on Th2 over Th1 cells. Using specific agonists, it has been demonstrated that the PGD<sub>2</sub>-mediated activation and migration of eosinophils, basophils and Th2 cells in vitro proceeds selectively via CRTh2 receptor activation. An emerging body of evidence of the activity of selective CRTh2 antagonists in pre-clinical rodent models supports this mechanism as a new therapeutic modality for treatment of asthma and other allergic diseases.<sup>3a,3b</sup>

Known drugs have been reported as ligands for the CRTh2 receptor (Fig. 1): ramatroban **1** is a thromboxane A<sub>2</sub> (TP) receptor antagonist used for treatment of allergic rhinitis in Japan which was shown to also exhibit CRTh2 antagonist activity<sup>4</sup> and the anti-inflammatory drug indomethacin **2** was described as an agonist of

CRTh2.<sup>5a,b</sup> Subsequently, related indoleacetic acid CRTh2 antagonist scaffolds have been reported such as **3**<sup>6</sup> and **4**<sup>7</sup> which were obtained by morphing approaches from indomethacin. A similar chemotype **5** was identified by optimisation of high throughput screening (HTS) hits.<sup>8</sup> A variety of other CRTh2 antagonist chemotypes have also been disclosed.<sup>9</sup> We conducted our own HTS to search for novel CRTh2 antagonists and have recently disclosed a series of 2-cycloalkylphenoxyacetic acids exemplified by **6** optimised from one hit series.<sup>10</sup> In this publication, we describe the optimisation of a 7-azaindole-3-acetic acid HTS hit **7** leading to compounds with improved potency and selectivity compared to **6**.

Compound **7** was identified as a potent ligand for the CRTh2 receptor in a [<sup>3</sup>H]-PGD<sub>2</sub> radioligand binding assay using CHO cells stably transfected with the human CRTh2 receptor. Functional activity was initially assessed using an isolated human eosinophil shape change (SC) assay as described previously.<sup>10</sup> An excellent level of selectivity was found for binding to the CRTh2 over the human DP and TP prostanoid receptors (Table 1). Most encouragingly, despite the structural similarity to indomethacin, less than 50% inhibition of ovine COX-1 or human COX-2 enzymes at 10 μM was observed. Against a broad panel of 46 G-protein coupled receptors (GPCRs) and 23 kinases no inhibition >50% at 10 μM concentration was noted. Initial assessment of biopharmaceutical properties (Table 2) indicated good solubility combined

\* Corresponding author.

E-mail address: [david.sandham@novartis.com](mailto:david.sandham@novartis.com) (D.A. Sandham).

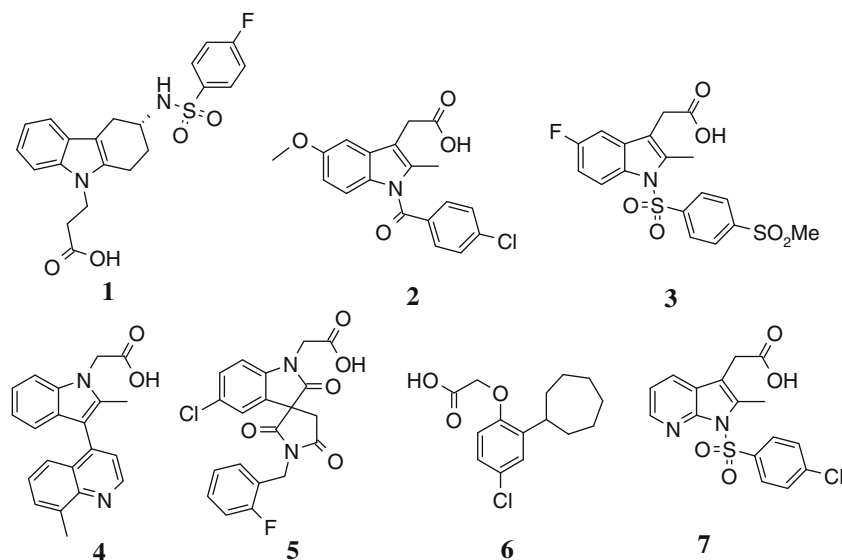


Figure 1. Selected ligands for the CRTh2 receptor.

Table 1  
On target and initial selectivity profiling of HTS hit 7

CRTh2 binding $K_i$ ( $\mu\text{M}$ )	Eosinophil SC $\text{IC}_{50}$ ( $\mu\text{M}$ )	DP binding $K_i$ ( $\mu\text{M}$ )	TP binding $K_i$ ( $\mu\text{M}$ )	COX-1 enzyme $\text{IC}_{50}$ ( $\mu\text{M}$ )	COX-2 enzyme $\text{IC}_{50}$ ( $\mu\text{M}$ )
0.103	0.108	>10	>10	>10	>10

$K_i$  and  $\text{IC}_{50}$  values represent the mean of at least two experiments.

Table 2  
Biopharmaceutical properties of HTS hit 7

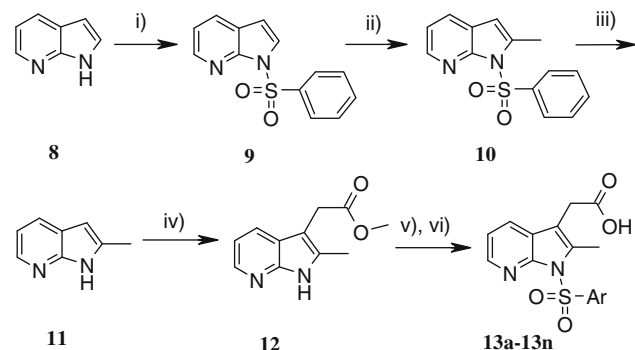
pH 6.8 Solubility (g/L)	HLM $\text{Cl}_{\text{int}}$ ( $\mu\text{L min mg}^{-1}$ )	RLM $\text{Cl}_{\text{int}}$ ( $\mu\text{L min mg}^{-1}$ )	Caco-2 permeability A-B/B-A ( $10^{-6}$ cm/s)
0.877	20	27	8.9/11.2

HLM: human liver microsomes; RLM: rat liver microsomes.

with moderate clearance and permeability. Taken together with the potency and selectivity data, this favourable profiling outcome encouraged us to initiate an optimisation programme to explore the structure–activity relationship (SAR) of the 7-azaindole-3-acetic acid scaffold.

An optimised route to the core structure is depicted in Scheme 1. Commercial 7-azaindole **8** was readily metallated and alkylated in the 2-position after N-sulfonylation. The activating group could be subsequently cleaved under mild conditions as described.<sup>11</sup> Installation of the acetate side chain was achieved directly by alkylation of a zincate species derived from **11** in a one pot procedure.<sup>12</sup> The resultant building block **12** was amenable to parallel array chemistry using a one pot sulfonylation–saponification protocol employing the phosphazene base BEMP. Upon scale-up of selected compounds for further profiling (e.g., **13f**), it was found that the use of NaH as base for sulfonylation and isolation of the resultant sulfonyl ester followed by Lewis acid-mediated ester cleavage gave improved yields.

A Topliss tree type<sup>13</sup> optimisation approach (Table 3) indicated a preference for electron deficient substituents on the aromatic ring and quickly lead us to **13f** as a candidate for further profiling. This compound retained antagonist activity in the eosinophil SC assay ( $\text{IC}_{50}$  0.112  $\mu\text{M}$ ). The results of rat pharmacokinetic (PK) studies on **13f** are shown in Table 4 and Figure 2, in which we were pleased to note low clearance and excellent oral bioavailability. In



Scheme 1. Representative syntheses of final compounds. Reagents and conditions: (i)  $\text{PhSO}_2\text{Cl}$ ,  $\text{BnEt}_3\text{NCl}$ ,  $\text{NaOH}$ ,  $\text{CH}_2\text{Cl}_2$ , rt, 80%; (ii)  $\text{LDA}$ ,  $\text{THF}$ ,  $\text{MeI}$ ,  $-78^\circ\text{C}$ , 90%; (iii)  $\text{TBAF}$ ,  $\text{THF}$ , rt, 75%; (iv)  $n\text{-BuLi}$ ,  $\text{THF}$ ,  $0^\circ\text{C}$ ;  $\text{ZnCl}_2$ ,  $0^\circ\text{C}$ ; evaporate; methyl bromoacetate, toluene,  $95^\circ\text{C}$ , 33%; (v)  $\text{ArSO}_2\text{Cl}$ ,  $\text{DMF}$ ,  $\text{BEMP}$ , rt or  $\text{ArSO}_2\text{Cl}$ ,  $\text{NaH}$ ,  $\text{THF}$ ,  $0^\circ\text{C}$ ; (vi) aq  $\text{NaOH}$  or  $\text{BBR}_3$ ,  $\text{CH}_2\text{Cl}_2$ , rt.

addition, the compound displayed reasonable flux across human Caco-2 cells. It could be speculated that the prolonged terminal half life (Fig. 2) and high volume of distribution were consequences of enterohepatic recirculation of either a putative acyl glucuronide metabolite or unchanged drug,<sup>14</sup> although the metabolism of **13f** was not subjected to characterisation.

Because of the moderate throughput of the eosinophil shape change assay, we introduced a CRTh2 whole CHO cell cAMP functional assay as a pre-screen in our compound profiling flow chart. Given the carboxylic acid functionality present in this chemotype, we were also aware of the potential for plasma protein binding to impact potency.<sup>15</sup> We therefore included a protocol to spike the assay medium with 0.1% human serum albumin (HSA) as an indirect measure of plasma protein binding. As shown in Figure 3, post

**Table 3**  
Optimisation of CRTh2 binding potency

Ar								
CRTh2 $K_i$ ( $\mu\text{M}$ )	0.377	3.22	0.282	2.619	0.619	0.052	1.171	0.048

$K_i$  values represent the mean of at least two experiments.

**Table 4**  
Rat PK and human permeability profile of compound **13f**

$T_{1/2}$ (iv, 1 mg/kg)	44.3 h
Cl	4.0 mL/min/kg
$V_{ss}$	9.8 L/kg
$F_{(po, 3 \text{ mg/kg})}$	100%
AUC (0–48 h)	2622 $\mu\text{M min}$
$C_{max}$	1.5 $\mu\text{M}$
Caco-2 A–B/B–A ( $10^{-6}$ cm/s)	8.7/19.3

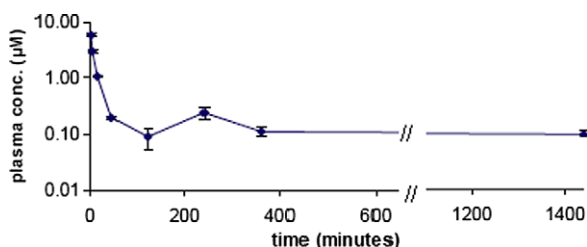


**Figure 2.** Rat intravenous PK plasma timecourse for compound **13f**. Data represents  $n = 3$ ,  $\pm$ SEM; lower limit of quantitation 10 nM.

*facto* analysis of a broader set of 7-azaindole-3-acetic acid analogues indicated a good correlation between eosinophil shape change and cAMP (+HSA) potency. A further development of the

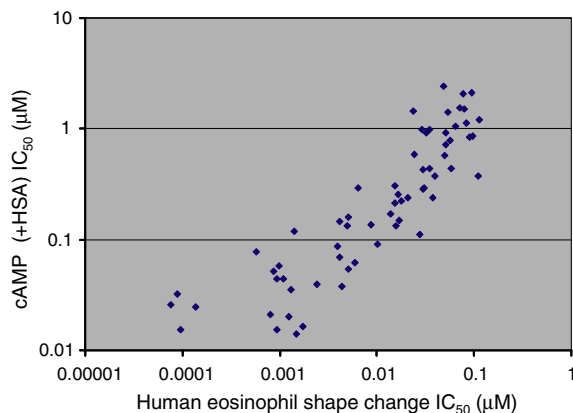


**Figure 3.** Correlation of eosinophil shape change potency with cAMP functional potency in the presence of HSA.



**Table 5**  
Comparison of **13f** with previous lead **6** and ramatroban **1**

	<b>6</b>	<b>13f</b>	<b>1</b>
CRTh2 binding $K_i$ ( $\mu\text{M}$ )	0.059	0.052	0.073
CRTh2 cAMP $\text{IC}_{50}$ ( $\mu\text{M}$ )	0.148	0.354	0.210
CRTh2 cAMP + HSA, potency shift	24	3.4	1.6
Eosinophil SC $\text{IC}_{50}$ ( $\mu\text{M}$ )	0.248	0.112	0.021
HWB SC $\text{IC}_{50}$ ( $\mu\text{M}$ )	>10	0.629	0.195
Human PPB <sup>a</sup>	99.4%	93.4%	96.1%
$\log D_{6,8}$ <sup>b</sup>	1.5	0.8	1.1

<sup>a</sup> Determined by HSA column HPLC method.<sup>16</sup>

<sup>b</sup> Determined from  $\log P$ <sup>17</sup> and predicted  $\text{pK}_a$ <sup>18</sup> values.

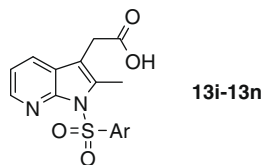
eosinophil shape change assay was implemented by conducting the assay in human whole blood (HWB). This delivered a more physiologically relevant environment, factoring in binding of compounds to plasma and other proteins, as well as providing a potential ex-vivo receptor occupancy assay suitable for a clinical setting. In this context, **13f** was compared with **7** from our earlier CRTh2 antagonist chemotype<sup>10</sup> and the reference dual CRTh2-TP antagonist ramatroban. We were encouraged to note that **13f** showed greatly improved functional potency in whole blood, despite similar binding and reduced functional cAMP activity compared to **6**, although it was inferior to ramatroban in both isolated and HWB eosinophil shape change assays (Table 5).

We speculated that reducing plasma protein binding (PPB) within the azaindole chemotype might be a key factor in delivering optimal whole blood potency. Within congeneric series of acidic compounds, there is thought to be a correlation between the extent of plasma protein binding and lipophilicity.<sup>19</sup> Accordingly, a small array of 3,4-disubstituted analogues of **13f** with reduced lipophilicity was prepared to probe this hypothesis. As shown in Table 6, reduction of  $\log D$  maintained binding activity, attenuated to some extent the potency loss in the presence of HSA, and improved isolated eosinophil SC potency. In the HWB eosinophil SC assay, we were pleased to identify **13l**, **13m** and **13n** with greatly improved potency compared to ramatroban.

Compounds **13l–n** were selected for further profiling in rat PK experiments (Table 7). The clearance of all compounds was increased compared to **13f**, and while **13l** showed moderate bioavailability, **13m** had poor exposure and **13n** could not be detected in plasma after oral dosing. For both **13l** and **13m**, significant levels of parent compound (9.1  $\mu\text{M}$  and 0.6  $\mu\text{M}$ , respectively) were found in urine collected up to 6 h post iv dosing, suggesting that oxidative metabolism played a minor role in their clearance. These compounds were also stable in rat plasma over 2 h, whereas **13n**

**Table 6**

Optimisation of eosinophil shape change potency



Ar						
	<b>13i</b>	<b>13j</b>	<b>13k</b>	<b>13l</b>	<b>13m</b>	<b>13n</b>
CRTh2 $K_i$ ( $\mu\text{M}$ )	0.158	0.056	0.043	0.031	0.035	0.036
cAMP $\text{IC}_{50}$ ( $\mu\text{M}$ )	0.311	0.091	0.031	0.060	0.041	0.101
HSA shift	1.8	2.4	1.7	1.3	1.8	1.0
Eosinophil SC $\text{IC}_{50}$ ( $\mu\text{M}$ )	0.050	0.018	0.005	0.009	0.006	0.008
HWB SC $\text{IC}_{50}$ ( $\mu\text{M}$ )	nd	0.156	nd	0.017	0.056	0.040
$\log D_{6.8}^a$	0.3	0.1	-0.3	-0.3	-0.6	-1.0

$K_i$  and  $\text{IC}_{50}$  values represent the mean of at least two experiments.  
nd not determined.

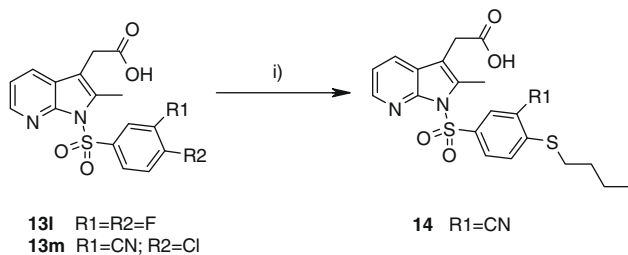
<sup>a</sup> Determined from  $\log P^{17}$  and predicted  $\text{p}K_a^{18}$  values.

**Table 7**Rat PK and permeability profiles of **13l-n**

	<b>13l</b>	<b>13m</b>	<b>13n</b>
$T_{1/2}$ (iv, 1 mg/kg) (h)	1.8	0.17	0.21
Cl (mL/min/kg)	20	67	52
$V_{ss}$ (L/kg)	4.9	0.3	4.1
$F$ (po, 3 mg/kg)	54%	8%	0%
AUC (0–48 h) ( $\mu\text{M min}$ )	222	12	—
$C_{max}$ ( $\mu\text{M}$ )	0.32	0.30	—
Rat plasma $T_{1/2}$ (mins)	>120	>120	55
Caco-2 A–B/B–A ( $10^{-6}$ cm/s)	9.5/8.8	1.0/4.4	1.4/0

exhibited significant instability in rat plasma in vitro, which may have contributed to the lack of exposure of the latter compound. In addition, the decreased lipophilicity of **13m** and **13n** may also have led to the observed reduced flux across Caco-2 cells<sup>20</sup> as a further contributory factor in the poor PK profiles of these compounds.

Mindful of the potential for *ipso* aromatic substitution on the 4-halobenzenesulfonamide moiety as a potential source of covalent adduct formation and possible toxicity,<sup>21</sup> we screened for the reactivity of **13l** and **13m** with *n*-butanethiol (Scheme 2). No reaction with either compound was observed in the absence of base, while in the presence of  $\text{K}_2\text{CO}_3$ , **13l** remained inert over 6 h, whereas **13m** showed 87% conversion by LC–MS to the sulfide adduct **14**. Interestingly, when **13l** and **13m** were incubated with human liver microsomes in the presence of the physiological sulfur nucleophile glutathione, no evidence of adduct formation with either compound could be detected by LC–MS.

**Scheme 2.** Reagents and conditions: (i) butanethiol,  $\text{K}_2\text{CO}_3$ , MeCN, rt, 6 h.

Compound **13l**<sup>22</sup> was further profiled as an advanced lead candidate and showed  $\text{IC}_{50} > 10 \mu\text{M}$  against a prostanoid receptor panel (DP, EP<sub>2</sub>, EP<sub>3</sub>, EP<sub>4</sub>, FP and TP receptors) and was also inactive ( $\text{IC}_{50} > 10 \mu\text{M}$ ) in COX-1 and COX-2 enzyme inhibition assays. The only significant activity in a broader panel of 46 GPCRs and 19 kinases was on CCK<sub>a</sub> ( $\text{IC}_{50}$  8.1  $\mu\text{M}$ ). In addition, the compound was tested for activity at the murine CRTh2 receptor stably transfected into K562 cells, where a  $K_i$  value of 28 nM for displacement of <sup>3</sup>[H]-PGD<sub>2</sub> was determined. In a GTP- $\gamma$ S functional assay using the same cell line, **13l** behaved as a functional antagonist ( $\text{IC}_{50}$  167 nM), confirming its suitability for potential use in mouse models of CRTh2-driven diseases. Further characterisation data was obtained as indicated in Table 8, indicating minimal potential for cardiotoxicity via hERG blockade and a low risk for drug–drug interactions arising from inhibition of the major cytochrome-P450 (CYP) isoforms. In addition, there was no activity found in the standard pre-clinical genetic toxicology assays, human plasma protein binding was relatively low, the compound was stable in a human liver microsomes clearance assay, as well as being highly soluble.

In conclusion, HTS identified a novel 7-azaindole-3-acetic acid chemotype as selective CRTh2 antagonists. The SAR of the scaffold was explored, and further optimisation based on reducing lipophilicity and plasma protein binding resulted in identification of compound **13l** as a potent and highly selective functional antagonist of the human CRTh2 receptor in human whole blood, exhibit-

**Table 8**Further profiling of compound **13l**

hERG patch clamp	16% Inhibition (10 $\mu\text{M}$ )
CYP1A2	$\text{IC}_{50} > 10 \mu\text{M}$
CYP2C9	$\text{IC}_{50} > 10 \mu\text{M}$
CYP2C19	$\text{IC}_{50} > 10 \mu\text{M}$
CYP2D6	$\text{IC}_{50} > 10 \mu\text{M}$
CYP3A4	$\text{IC}_{50} > 10 \mu\text{M}$
Ames test <sup>a</sup>	Negative
TK6 human micronucleus assay	Negative
Human plasma protein binding <sup>b</sup>	89.8%
Human liver microsomes $\text{Cl}_{int}$	0 $\mu\text{L min}^{-1} \text{mg}^{-1}$
pH 6.8 buffer thermodynamic solubility	>6 g/L

<sup>a</sup> In the presence and absence of S9 liver microsomes.

<sup>b</sup> By HSA column method.<sup>17</sup>

ing oral bioavailability in the rat and generally favourable drug-like properties. Further optimisation of **131** and analogues<sup>23a–c</sup> towards clinical candidates will be disclosed in due course.

## References and notes

- Murray, J. J.; Tonnel, A. B.; Brash, A. R.; Roberts, L. J.; Gosset, P.; Workman, R.; Capron, A.; Oates, J. A. *N. Engl. J. Med.* **1986**, *315*, 800.
- Pettipher, R.; Hansel, T. T.; Armer, R. *Nat. Rev. Drug Disc.* **2007**, *6*, 313.
- (a) Lukacs, N. W.; Berlin, A. A.; Franz-Bacon, K.; Sasik, R.; Sprague, L. J.; Ly, T. W.; Hardiman, G.; Boehme, S. A.; Bacon, K. B. *Am. J. Physiol.* **2008**, *295*, L767; (b) Boehme, S. A.; Franz-Bacon, K.; Chen, E. P.; Sasik, R.; Sprague, L. J.; Ly, T. W.; Hardiman, G.; Bacon, K. B. *Int. Immunol.* **2009**, *21*, 81.
- Sugimoto, H.; Shichijo, M.; Iino, T.; Manabe, Y.; Watanabe, A.; Shimazaki, M.; Gantner, F.; Bacon, K. B. *J. Pharmacol. Exp. Therap.* **2003**, *305*, 347.
- (a) Sawyer, N.; Cauchon, E.; Chateaufneuf, A.; Cruz, R. P. G.; Nicholson, D. W.; Metters, K. M.; O'Neill, G. P.; Gervais, F. G. *Br. J. Pharmacol.* **2002**, *13*, 1163; (b) Hirai, H.; Tanaka, K.; Takano, S.; Ichimasa, M.; Nakamura, M.; Nagata, K. *J. Immunol.* **2002**, *168*, 981.
- Armer, R. E.; Ashton, M. R.; Boyd, E. A.; Brennan, C. J.; Brookfield, F. A.; Gazi, L.; Gyles, S. L.; Hay, P. A.; Hunter, M. G.; Middlemiss, D.; Whittaker, M.; Xue, L.; Pettipher, R. *J. Med. Chem.* **2005**, *48*, 6174.
- Birkinshaw, T. N.; Teague, S. J.; Beech, C.; Bonnett, R.; Hill, S.; Patel, A.; Reakes, S.; Sangane, H.; Dougall, I. G.; Phillips, T. T.; Salter, S.; Schmidt, J.; Arrowsmith, E. C.; Carrillo, J. J.; Bell, F. M.; Paine, S. W.; Weaver, R. *Bioorg. Med. Chem. Lett.* **2006**, *16*, 4287.
- Crosignani, S.; Page, P.; Missotten, M.; Colovray, V.; Cleva, C.; Arrighi, J.-F.; Atherall, J.; Macritchie, J.; Martin, T.; Humbert, Y.; Gaudet, M.; Pupowicz, D.; Maio, M.; Pittet, P.-A.; Golzio, L.; Giachetti, C.; Rocha, C.; Bernardinelli, G.; Filinchuk, Y.; Scheer, A.; Schwarz, M. K.; Chollet, A. *J. Med. Chem.* **2008**, *51*, 2227.
- Medina, J. C.; Liu, J. *Ann. Rep. Med. Chem.* **2006**, *41*, 221.
- Sandham, D. A.; Aldcroft, C.; Baettig, U.; Barker, L.; Beer, D.; Bhalay, G.; Brown, Z.; Dubois, G.; Budd, D.; Bidlake, L.; Campbell, E.; Cox, B.; Everatt, B.; Harrison, D.; Leblanc, C. J.; Manini, J.; Profit, R.; Stringer, R.; Thompson, K. S.; Turner, K. L.; Tweed, M. F.; Walker, C.; Watson, S. J.; Whitebread, S.; Willis, J.; Williams, G.; Wilson, C. *Bioorg. Med. Chem. Lett.* **2007**, *17*, 4347.
- Desarbre, E.; Coudret, S.; Meheust, C.; Merour, J.-Y. *Tetrahedron* **1997**, *53*, 3637.
- McKew, J. C.; Foley, M. A.; Thakker, P.; Behnke, M. L.; Lovering, F. E.; Sum, F.-W.; Tam, S.; Wu, K.; Shen, M. W. H.; Zhang, W.; Gonzalez, M.; Liu, S.; Mahadevan, A.; Sard, H.; Khor, S. P.; Clark, J. D. *J. Med. Chem.* **2006**, *49*, 135.
- Topliss, J. G. *J. Med. Chem.* **1972**, *15*, 1006.
- Roberts, M. S.; Magnusson, B. M.; Burczynski, F. J.; Weiss, M. *Clin. Pharmacokinet.* **2002**, *41*, 751.
- Young, R. N. *Prog. Med. Chem.* **2001**, *38*, 249.
- Valko, K.; Nunhuck, S.; Bevan, C.; Abraham, M. H.; Reynolds, D. P. *J. Pharm. Sci.* **2003**, *92*, 2236.
- Values calculated using CLOGP v4.71, BioByteCorp, Claremont, CA, USA.
- Jelfs, S.; Ertl, P.; Selzer, P. *J. Chem. Inf. Model.* **2007**, *47*, 450.
- Kratochwil, N. A.; Huber, W.; Mueller, F.; Kansy, M.; Gerber, P. R. *Curr. Opin. Drug Discovery Dev.* **2004**, *7*, 507.
- Waring, M. J. *Bioorg. Med. Chem. Lett.* **2009**, *19*, 2844.
- Zhou, S.; Chan, E.; Duan, W.; Huang, M.; Chen, Y.-Z. *Drug Metab. Rev.* **2005**, *37*, 41.
- Selected data for **131**:  $\delta_{\text{H}}$  (400 MHz, DMSO- $d_6$ ) 2.62 (3H, s), 3.69 (2H, s), 7.28 (1H, dd,  $J$  7.8, 4.8), 7.69 (1H, dd,  $J$  17.6, 9.1), 7.92 (1H, dd,  $J$  7.8, 1.5), 8.06 (1H, m), 8.26 (1H, ddd,  $J$  9.8, 7.2, 2.4), 8.32 (1H, dd,  $J$  4.8, 1.5) (12.48, 1H, br s);  $\delta_{\text{F}}$  ( $^1\text{H}$ ) (377 MHz, DMSO- $d_6$ ) -134, -128;  $m/z$  (APCI +ve) 367;  $\text{C}_{16}\text{H}_{12}\text{F}_2\text{N}_2\text{O}_4\text{S}$  requires C, 52.38; H, 3.1; N, 10.78; S, 8.23. Found C, 52.76; H, 3.353; N, 10.46; S, 8.053.
- (a) Bala, K.; Leblanc, C.; Sandham, D.A.; Turner, K. L.; Watson, S.J.; Brown, L.N.; Cox, B. PCT Int. Appl. WO2005123731, 2005; *Chem. Abstr.* **2005**, *144*, 88269; (b) Brown, L.N.; Leblanc, C.; Sandham, D.A.; Singh, H.P.; PCT Int. Appl. WO 2007065683, 2007; *Chem. Abstr.* **2007**, *147*, 72640; (c) Sandham, D.A. PCT Int. Appl. WO2007065684, 2007; *Chem. Abstr.* **2007**, *147*, 72634.